Nucleon Resonances in Meson Nucleon Scattering with Strangeness Production

A. Waluyo [a*], C. Bennhold[a*], H. Haberzettl[a*], G. Penner [b†], U. Mosel[b†], and T. Mart[c‡]

[a]Center for Nuclear Studies, Department of Physics, The George Washington University, Washington, D.C. 20052, USA

[b]Institut für Theoretische Physik, Universität Giessen, D-35392 Giessen, Germany.

[c]Jurusan Fisika, FMIPA, Universitas Indonesia, Depok 16424, Indonesia

An effective Lagrangian model in a coupled channels framework is applied to extract nucleon resonance parameters. In the K-matrix approximation, we simultaneously analyze all the available data for the transitions from πN to five possible meson-baryon final states, $\pi N, \pi\pi N, \eta N, K\Lambda$, and $K\Sigma$, in the energy range from πN threshold up to $\sqrt{s} = 2$ GeV. In this work, we focus our efforts on the $K\Sigma$ channel. In particular, we include a set of Δ resonances around 1900 MeV: the $S_{31}(1900), P_{31}(1910)$, and $P_{33}(1920)$ states. In most cases the parameters of nucleon resonances determined by the fits are consistent with the commonly accepted values in the literature. We find that in the low-energy region, the $S_{11}(1650), P_{11}(1710)$, and $P_{13}(1720)$ states are important for the $p(\pi^-, K^0)\Sigma^0$ and $p(\pi^-, K^+)\Sigma^-$ processes while the $P_{33}(1600)$ and $D_{33}(1700)$ states are significant for the pure I=3/2 reaction $p(\pi^+, K^+)\Sigma^+$. In the high energy region, we find a D_{13} state at 1945 MeV which is important for the $p(\pi^-, K^0)\Sigma^0$ reaction while the Δ resonances around 1900 MeV show up significantly in the $p(\pi^-, K^+)\Sigma^-$ and $p(\pi^+, K^+)\Sigma^+$ processes.

1. INTRODUCTION

The study of nucleon resonances continues to challenge the field of hadronic physics. The interest in this field has grown significantly in the last few years because of new data from experimental facilities such as Jefferson Lab, ELSA, MAMI, and Brookhaven National Laboratory.

Nucleon resonances are usually identified in πN partial waves analyses, where they are labeled by the approximate mass and the πN quantum numbers, which are the relative orbital angular momentum L, the total isospin T and the total angular momentum J. For example, the $D_{13}(1520)$ resonance has a mass of about 1520 MeV, isospin $T = 1/2$, total angular momentum $J = 3/2$ and decays into an $L = 2$ πN state.

There are about 20 $N^*(T = 1/2)$ and 20 $\Delta(T = 3/2)$ resonance states in the 1998 PDG

*Supported in part by US DOE with grant no. DE-FG02-95ER-40907
†Supported by DFG and GSI Darmstadt (Germany)
‡Supported in part by the University Research for Graduate Education (URGE) grant.

publication [1]. Some of these have well established properties, while for others there are still large discrepancies between different analyses. One example is the $S_{11}(1535)$ state. Even though this state has been given a 4-star label from PDG [1] the extracted total and partial widths of this state differ widely for different analyses [2–4].

The study of nucleon resonances generally takes place in two theoretical arenas. There are model studies using the assumption that nucleons and their excited states are composed primarily of three valence quarks [5–7]. In recent years, lattice QCD calculations have been extended to predict masses of the low-lying baryons [8]. Although lattice QCD calculations are powerful to determine mass spectra they are more difficult to apply to decay widths. In order to provide a link between the new and improved data on the one side and the results from lattice QCD and quark models on the other side, dynamical descriptions using hadronic degrees of freedom are required to analyze the data in the various asymptotic reaction channels, like $\gamma N, \pi N, \pi\pi N, \eta N, K\Lambda, K\Sigma$, and others.

Clearly, the principal problem faced in this undertaking is the number of open channels. With more than one open channel in a meson production reaction the unknown couplings, masses and widths of the resonances can only be obtained if all open channels are treated simultaneously, thus maintaining unitarity.

In order to study the structure of nucleon resonances in the higher energy region, one needs to include strangeness production channels like $K\Lambda$ and $K\Sigma$. Usually models that study these channels [9] neglect the hadronic final state interaction, performing calculations at tree level. Clearly, this leads to a violation of unitarity. Unitarity can only be maintained dynamically if we solve the coupled channels system including all possible channels, such as $\eta N \to K\Lambda$, for which no experimental data are available.

In this study we extend the model of Feuster and Mosel [3] by including the previously neglected $K\Sigma$ final state. We furthermore extend the energy range to $\sqrt{s} \leq 2.0$ GeV, thus including several additional resonanes between 1.9 GeV $\leq \sqrt{s} \leq 2.0$ GeV. All 2π final states like ρN and $\Delta\pi$ continue to be parametrized through the coupling to a scalar, isovector ζ-meson with mass $m_\zeta = 2m_\pi$.

2. Model for Meson Nucleon Scattering

In general, the scattering amplitude of meson nucleon scattering can be written in terms of a Bethe-Salpeter equation

$$T_{\varphi,\varphi} = V_{\varphi,\varphi}(k', q, P) + i \int \frac{d^4k"}{(2\pi)^4} V_{\varphi,\varphi}(k', k", P) G_{BS}(k", P) T_{\varphi,\varphi}(k", q, P) \tag{1}$$

where φ stands for $\pi, \eta, \pi\pi$, or K, and $V_{\varphi\varphi}(k', q, P)$ is the driving potential. The four momenta for the incoming, outgoing, and intermediate nucleons are p, p', and $p"$, of the outgoing and intermediate mesons are k' and $k"$, and of the incoming meson is q, so that $P = p + q = p' + k' = p" + k"$ is the total four-momentum. $G_{BS}(k, P)$ is the full Feynman meson-baryon propagator and is defined as follows

$$G_{BS}(k, P) = \frac{m + \not{P}' - \not{k}}{(\mu^2 - k^2 - i\epsilon)(m^2 - (P - k)^2 - i\epsilon)}. \tag{2}$$

In principle, one needs to solve the Bethe-Salpeter equation in its four-dimensional integral form. In practice, approximations are used to obtain solutions.

2.1. The K-matrix approximation

The Bethe-Salpeter equation can always be decomposed into two equations:

$$\begin{aligned} K &= V + V\mathrm{Re}(G_{BS})K, \\ T &= K - \mathrm{i}K\mathrm{Im}(G_{BS})T. \end{aligned} \tag{3}$$

If we choose to put the intermediate particle on-shell, i.e. neglecting the real part of G_{BS}, we get

$$iG_{\mathrm{K}} = -2i(2\pi)^2 m_N \delta(k_N^2 - m_N^2)\delta(k_m^2 - m_m^2) \times \ \theta(k_N^0)\theta(k_m^0)(\not{k}_N + m_N) \tag{4}$$

from which we obtain $K = V$ and thus the K-matrix Born approximation.

$$[T_K] = [V + \mathrm{i}VT_K] = \left[\frac{V}{1 - \mathrm{i}V}\right], \tag{5}$$

where the brackets denote that we have to deal with matrices containing all allowed final state combinations.

2.2. Background contributions

Our model contains contributions from the standard Born terms, the $t-$channel exchange via ρ, a_0, and K^* and the resonance contributions in the $s-$ and $u-$channels. The potential V is calculated from the interaction Lagrangian below. For the Born and t-channel couplings we have:

$$\begin{aligned} \mathcal{L}_{NR} = &- \frac{g_{\varphi NN}}{2m_N}\bar{N}\gamma_5\gamma_\mu(\partial^\mu\varphi)N - g_{sNN}s(\bar{N}N) - g_{s\varphi\varphi}s(\varphi^*\varphi) \\ &- g_{vNN}\bar{N}\left(\gamma_\mu v^\mu - \kappa_v\frac{\sigma_{\mu\nu}}{4m_N}v^{\mu\nu}\right)N - g_{v\varphi\varphi}\left[\varphi \times (\partial_\mu\varphi)\right]v^\mu, \end{aligned} \tag{6}$$

φ denotes the asymptotic mesons π, η, and K. A coupling to the ζ-meson is not taken into account. s and v are the intermediate scalar and vector mesons (a_0, ρ, K_0^* and K^*) and $v^{\mu\nu} = \partial^\nu v^\mu - \partial^\mu v^\nu$ is the field tensor of the vector mesons. N is either a nucleon, Λ, or a Σ spinor. For $I = 1$ mesons (π and ρ) φ and v^μ need to be replaced by $\boldsymbol{\tau}\cdot\boldsymbol{\varphi}$ and $\boldsymbol{\tau}\cdot\boldsymbol{v}^\mu$ in the φ, vNN-couplings.

3. Results of the Fits to Hadronic Data

We performed a fit to all hadronic data for the reactions $\pi N \to \pi N$, $\pi N \to \pi\pi N$, $\pi N \to \eta N$, $\pi N \to K\Lambda$, and $\pi N \to K\Sigma$ up to an energy of W = 2.0 GeV. The results of the Born couplings are displayed in table 2. We point out that the $g_{K\Lambda N}$ and $g_{K\Sigma N}$ couplings are in accordance with approximate SU(3), in contrast to ref. [3] which found a much smaller $g_{K\Lambda N}$ coupling constant. In addition to ref. [3] we allow contributions from the $S_{31}(1900), P_{31}(1910)$ and $P_{33}(1920)$ Δ resonances. Our best fit results in three D_{13}

excitations, the well-known $D_{13}(1520)$ state, the 3-star $D_{13}(1700)$ state and a new D_{13} state at 1945 MeV with a large width of 583 MeV. As discussed in detail in refs. [10,11], it is at present not clear if this D_{13} state corresponds to the 2-star resonance $D_{13}(2080)$ listed in the Particle Data Table. A closer examination of the literature reveals that there has been some evidence for two resonances in this partial wave between 1800 and 2200 MeV [4]; one with a mass centered around 1900 MeV and another with mass around 2080 MeV. It is the former which has been seen prominently in two separate $p(\pi^-, K^0)\Lambda$ analyses [12,13].

We now focus our discussion on the role of background versus nucleon resonant con-

Table 1
Extracted resonance parameters. ^{a}: The coupling constant is given instead of the partial width.

	M	Γ_{tot}	$\Gamma_{\pi N}$		$\Gamma_{\zeta N}$		$\Gamma_{\eta N}$		$\Gamma_{K\Lambda}$		$\Gamma_{K\Sigma}$	
$L_{2I,2S}$	[GeV]	[MeV]	[MeV]	%	[MeV]	%	[MeV]	%	[MeV]	%	[MeV]	%
$S_{11}(1535)$	1.547	244	89	36	9	4	146	60	-	-	-	-
$S_{11}(1650)$	1.689	341	189	55	71	22	1	0	80	23	0.98^a	0
$P_{11}(1440)$	1.473	434	282	65	152	35	3.84^a	0	-	-	-	-
$P_{11}(1710)$	1.716	235	0.43	0	76	32	54	23	73	31	32	14
$P_{13}(1720)$	1.736	137	33	25	77	56	18	13	2	1	7	5
$P_{13}(1900)$	1.951	300	80	27	213	71	0	0	5	2	2	0
$D_{13}(1520)$	1.507	93	51	55	42	45	0.003	0	-	-	-	-
$D_{13}(1700)$	1.706	86	0.52	0	33	38	42	49	10	12	1	1
$D_{13}(1900)$	1.945	583	108	19	439	75	28	5	8	1	0.08	0
$S_{31}(1620)$	1.616	148	56	38	92	62	-	-	-	-	-	-
$S_{31}(1900)$	1.938	334	121	36	166	50	-	-	-	-	47	14
$P_{31}(1910)$	1.967	605	119	20	452	74	-	-	-	-	34	6
$P_{33}(1232)$	1.229	110	110	100	-	-	-	-	-	-	-	-
$P_{33}(1600)$	1.677	296	44	15	252	85	-	-	-	-	0.59^a	0
$P_{33}(1920)$	2.077	689	114	17	575	83	-	-	-	-	0.60	0
$D_{33}(1700)$	1.672	583	73	13	510	87	-	-	-	-	0.31^a	0

Table 2
Couplings of the meson nucleon as obtained in the fits.

g	Value	g	Value	κ	Value
$g_{\pi NN}$	13.21	$g_{\rho NN}$	1.95	$\kappa_{\rho NN}$	2.29
$g_{KN\Sigma}$	1.41	$g_{K^*N\Sigma}$	-1.12	$\kappa_{K^*N\Sigma}$	-0.38
$g_{\eta NN}$	0.36	$g_{a_0 NN}$	0.98	-	-
$g_{KN\Lambda}$	-13.98	$g_{K^*N\Lambda}$	-4.96	$\kappa_{K^*N\Lambda}$	-0.37

tributions in the $K\Sigma$ channel at different energies. All resonance parameters we have extracted are given in table 1 which shows that nucleon resonances with the largest decay width into the $K\Sigma$ channel are the $P_{11}(1710), P_{13}(1720), S_{31}(1900)$, and $P_{31}(1910)$ states.

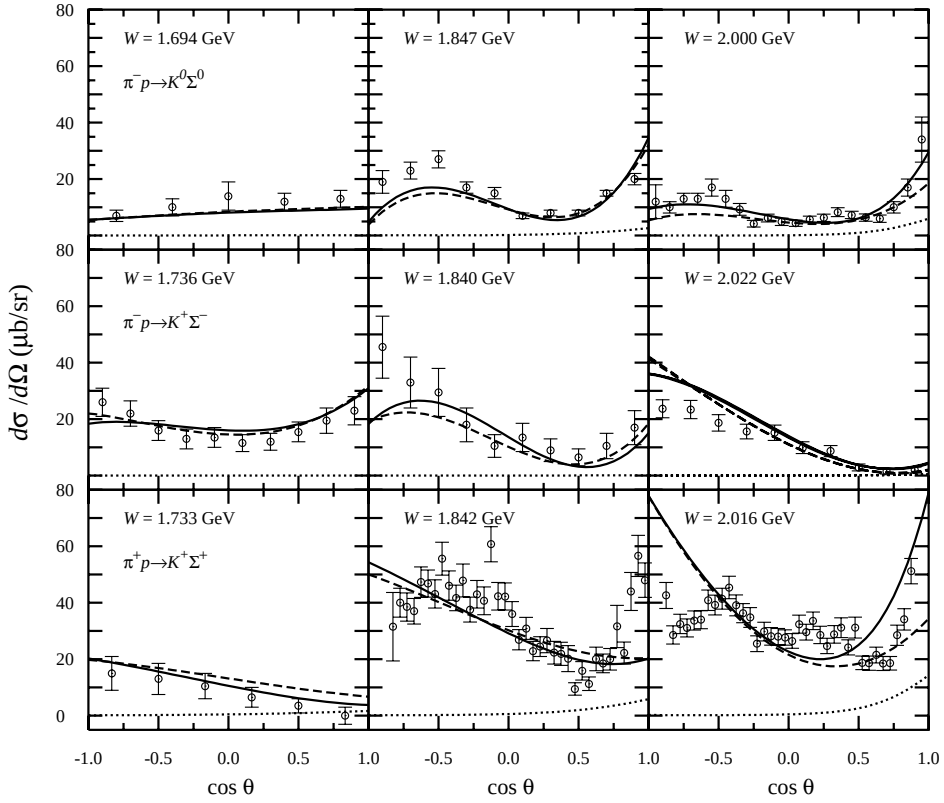

Figure 1. Differential cross sections of the three $\pi N \to K\Sigma$ reactions. Shown are the results from the full calculation (solid line), Born contributions only (dotted line), and the full calculation without K* (dashed line). The data are from ref. [16]

Figure 1 shows that the structure of the differential cross section for $\pi N \to K\Sigma$ is dominated by resonances. At higher energies we find forward peaking behavior from the $t-$channel K^* exchange. This can be seen especially in the $p(\pi^+, K^+)\Sigma^+$ reaction. This confirms what has been found in reference [3] about the role of vector meson $t-$channel exchange at higher energies.

In fig. 2 we examine the role of nucleon resonances in the low energy region. Since the extracted partial widths for $P_{11}(1710)$ and $P_{13}(1720)$ into the $K\Sigma$ channel are 32 and 73 MeV, one expects these resonances to have an important contribution in this energy region. For the $K^0\Sigma^0$ and $K^+\Sigma^-$ reactions, we find that the main contribution at low energies indeed comes from these two resonances. For the $p(\pi^-, K^+)\Sigma^-$ reaction, it can be seen clearly that the $P_{11}(1710)$ gives backward peaking behavior while the $P_{13}(1720)$ is responsible for forward peaking behavior. The role of the $P_{11}(1710)$ is consistent with recent studies of kaon photoproduction [14] and of $K\Sigma$ production in NN-scattering

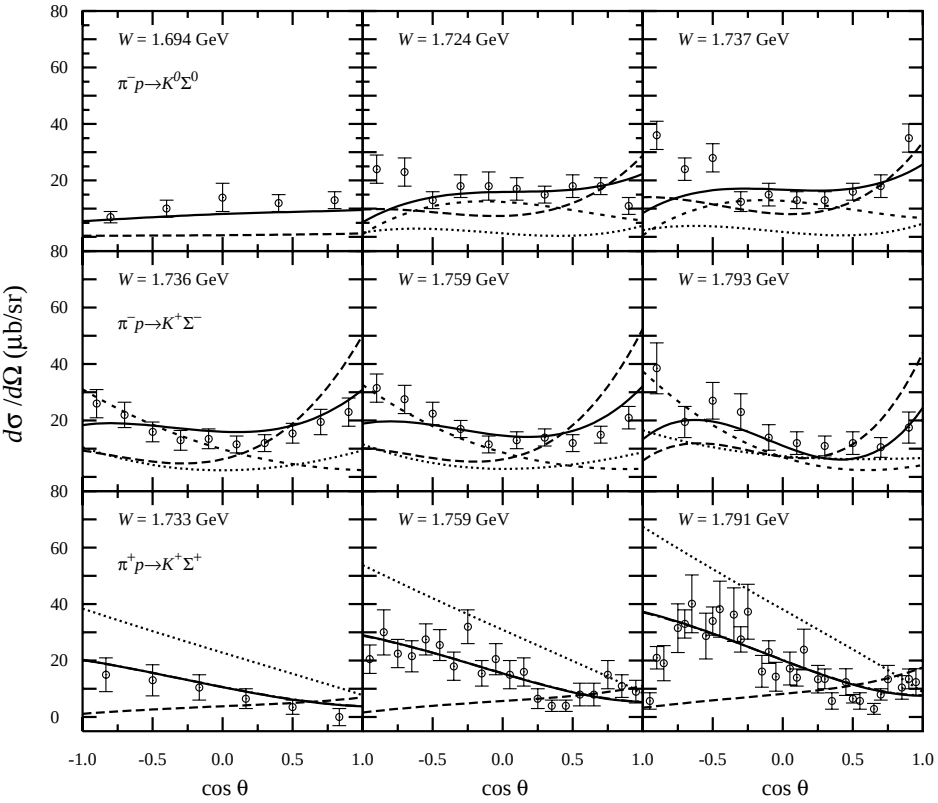

Figure 2. Differential cross sections of the three $K\Sigma$ reactions in the low energy region. Shown for the $p(\pi^-, K^0)\Sigma^0$ and $p(\pi^-, K^+)\Sigma^-$ reactions are the full calculation (solid line), without the $P_{11}(1710)$ (long-dashed line), without the $P_{13}(1720)$ (short-dashed line), and excluding both the $P_{11}(1710)$ and $P_{13}(1720)$ at the same time (dotted line). For $p(\pi^-, K^0)\Sigma^0$ at W = 1.694 GeV we only show the full calculation (solid line) and without the $S_{11}(1650)$ (dashed line). For the I=3/2 reaction $p(\pi^+, K^+)\Sigma^+$ we show the full calculation (solid line), without the $P_{33}(1600)$ (dashed line) and without the $D_{33}(1700)$ (dotted line).

[15], $NN \to NK\Sigma$, where the $P_{11}(1710)$ state was identified as a major contribution. Figure 2 also demonstrates that very close to threshold ($W_{threshold} = 1690$ MeV for $K^0\Sigma^0$ production) at $W_{cm} = 1694$ MeV, the structure of the differential cross section of the $p(\pi^-, K^0)\Sigma^0$ reaction comes mainly from the $S_{11}(1650)$ state. The extracted mass of this resonance is 1689 MeV, the total width is 341 MeV and the coupling constant to the $K\Sigma$ channel is 0.98. Even though this resonance lies below the threshold of the $p(\pi^-, K^0)\Sigma^0$ reaction, it is clearly its proximity to the $K^0\Sigma^0$ production threshold that leads to its dominating influence on the threshold cross section.

Now we come to the most interesting reaction in the $K\Sigma$ channel, which is $p(\pi^+, K^+)\Sigma^+$. This reaction is a pure isospin 3/2 process. Therefore, as expected, we do not see any effects of the $P_{11}(1710)$ and $P_{13}(1720)$ states. Fig. 2 shows that the effects of the $P_{33}(1600)$ and $D_{33}(1700)$ states are large in the low-energy region. The extracted masses

for the $P_{33}(1600)$ and $D_{33}(1700)$ are 1677 MeV and 1672 MeV, respectively, but their total widths are 296 MeV and 583 MeV which leads to broad resonance tails and significant influence on the cross section. From fig. 2 it is clear that the $D_{33}(1700)$ gives the largest contribution which interferes destructively with a smaller signal from the $P_{33}(1600)$.

In fig. 3 the $K\Sigma$ channel is studied at higher energies. The three Δ states, the $S_{31}(1900), P_{31}(1910)$, and $P_{33}(1920)$ are important in both isospin 1/2 and 3/2 channels.

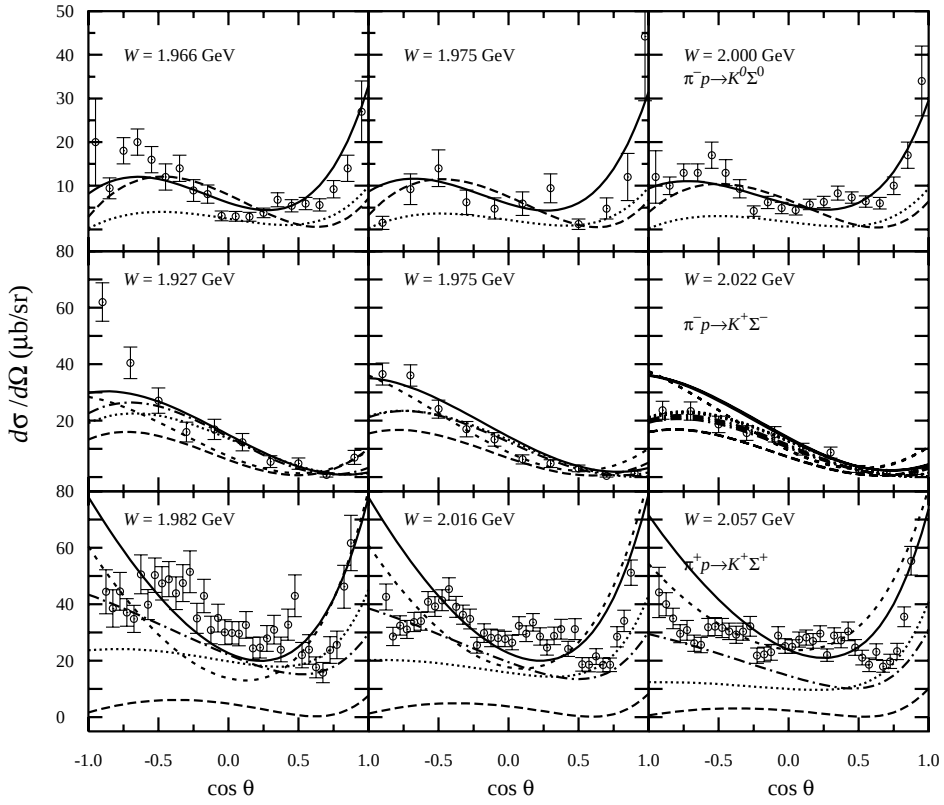

Figure 3. Differential cross sections of the three $K\Sigma$ reactions at higher energies. For all three reactions we display the full calculation (solid line) and results leaving out the $S_{31}(1900), P_{31}(1910)$, and $P_{33}(1920)$ states (long-dashed line). Furthermore, for the $p(\pi^-, K^0)\Sigma^0$ reaction we also show calculations without the $P_{13}(1900)$ (short-dashed line), and without the $D_{13}(1900)$ (dotted line). Finally, for the $p(\pi^-, K^+)\Sigma^-$ and $p(\pi^+, K^+)\Sigma^+$ reactions, calculations are displayed without the $S_{31}(1900)$ (short-dashed line), without the $P_{31}(1910)$ (dotted line) and without the $P_{33}(1920)$ (dot-dashed line).

For the $K^0\Sigma^0$ reaction, we find that the $S_{31}(1900), P_{31}(1910)$, and $P_{33}(1920)$ contribute only at forward angles. At backward angles we find that the main contribution to the cross section of this reaction comes from the $D_{13}(1900)$. For the $K^+\Sigma^-$ reaction, we find that the $S_{31}(1900)$ and $P_{31}(1910)$ supply the main contributions to the structure of the cross section. For the $K^+\Sigma^+$ reaction, all three Δ resonances build up the cross section. Even though the $P_{33}(1920)$ has only a small partial width into this channel ($\Gamma_{K\Sigma} = 593$ keV), its

role is significant in the backward angle region. The main contribution to the cross section comes from the $S_{31}(1900)$ and $P_{31}(1910)$. However, the model cannot reproduce the structure of the differential cross section data. This structure might come from high-spin N^* resonance contributions (such as spin 5/2 or 7/2) or different background mechanisms not included in the model.

4. Conclusion

We have investigated the role of nucleon resonances within a coupled channels framework. In the $K-$matrix approximation and with five allowed asymptotic states, $\pi N, \pi\pi N$, $\eta N, K\Lambda$, and $K\Sigma$, we fit the hadronic data in the energy range πN threshold up to $W_{cm} = 2$ GeV.

Focussing on the $K\Sigma$ channel we find that the structure of the differential cross section comes purely from resonance contributions. We also find that $P_{11}(1710)$ and $P_{13}(1720)$ give the main contributions to the cross section in the low energy region of the $p(\pi^-, K^0)\Sigma^0$ and $p(\pi^-, K^+)\Sigma^-$ reactions. At higher energies, the $D_{13}(1900)$ dominates the $p(\pi^-, K^0)\Sigma^0$ reaction while the $S_{31}(1900)$ and $P_{31}(1900)$ dominate the cross section for the $p(\pi^-, K^+)\Sigma^-$ reaction. For the $p(\pi^+, K^+)\Sigma^+$ reaction, we find no satisfactory mechanism in the high energy region, even though the $S_{31}(1900)$ and $P_{31}(1900)$ states play an important role in this regime. As the next step the photoproduction reaction $\gamma N \to K\Sigma$ will be studied along with the hadronic production reactions discussed here.

This work was supported by DOE grant DE-FG02-95ER-40907 (AW, CB, and HH), DFG and GSI Darmstadt (GP and UM), and a University Research for Graduate Education (URGE) grant (TM).

REFERENCES

1. Particle Data Group, *Eur. Phys. J.* **C3**, 1 (1998).
2. T.P. Vrana, S.A. Dytman and T.-S.H. Lee *Phys. Rep.* **328**, 181 (2000).
3. T. Feuster and U. Mosel *Phys. Rev.* **C58**, 457 (1998).
4. R. E. Cutkosky *et al.*, Phys. Rev. D **20**, 2839 (1979); G. Höhler, F. Kaiser, R. Koch, E. Pietarinen, Physics Data, No. 12-1 (1979).
5. N. Isgur and G. Karl, Phys. Lett. B **72**, 109 (1977); Phys. Rev. D **23**, 817 (1981); R. Koniuk and N. Isgur, Phys. Rev. D **21**, 1868 (1980).
6. S. Capstick and W. Roberts, Phys. Rev. D **49**, 4570 (1994).
7. S. Capstick and W. Roberts, Phys. Rev. D **58**, 074011 (1998).
8. F. X. Lee and D. B. Leinweber, Nucl. Phys. Proc. Suppl. **73**, 258 (1999) (hep-lat/9809095 (1998)).
9. R.A. Adelseck *et al. Phys. Rev.* **C42**, 108 (1990), J. C. David *et al. Phys. Rev.* **C53**, 2613 (1996), R. A. Williams *et al. Phys. Rev.* **C46**, 1617 (1992), T. Mart *et al. Phys. Rev.* **C51**, R1074 (1995).
10. T. Mart and C. Bennhold, Phys. Rev. C **61**, 012201(R) (1999).
11. C. Bennhold *et al.*, Proceedings of *NSTAR*2000, Jefferson Lab, Feb. 16-19, 2000 (in press).
12. D. H. Saxon *et al.*, Nucl. Phys. **B162**, 522 (1980).
13. K. W. Bell *et al.*, Nucl. Phys. **B222**, 389 (1983).

14. C. Bennhold *et al.* nucl-th/9901066.
15. A. Sibirtsev *et al.* nucl-th/9804070.
16. Baker, *Nucl. Phys.* **B145**, 402 (1978), Binford, *Phys. Rev.* **183**, 1134 (1969), Hart *Nucl. Phys.* **B166**, 73 (1979), O. I. Dahl *et al.*, *Phys. Rev.* **163**, 1430 (1967), M. L. Good, *Phys. Rev.* **183**, 1142 (1969), J. C. Doyle *et al.*, *Phys. Rev.* **165**, 1483 (1968), O. Goussu *et al.*, *Nuovo Cim.* **42A**, 606 (1966), M. Winnik, *Nucl. Phys.* **B128**, 66 (1977), Baltay, *Rev. Mod. Phys.* **33**, 374 (1961), Crawford, *Phys. Rev.* **128**, 368 (1962), Candlin, *Nucl. Phys.* **B226**, 1 (1983), Bellamy, *Phys. Lett.* **39B**, 299 (1972), Haba, *Nucl. Phys.* **B299**, 627 (1988).